Adsorption Reactions of Carboxylic Acid Functional Groups on Sodium Aluminoborosilicate Glass Fiber Surfaces

Joshua J. Stapleton,*,† Daniel L. Suchy,‡ Joy Banerjee,§ Karl T. Mueller,†,‡ and Carlo G. Pantano†,§

Materials Research Institute and Departments of Chemistry and Materials Science and Engineering, Pennsylvania State University, University Park, Pennsylvania 16802, United States

ABSTRACT Multicomponent silicate glasses are ubiquitous in modern society as evidenced by their inclusion in applications ranging from building materials and microelectronics to biomedical implants. Of particular interest in this study is the interface between multicomponent silicate glasses and adhesive polymers. These polymeric systems often possess a variety of different organic functional groups. In this study, we selected acetic acid as a probe molecule representative of the carboxylic acid functional group found in many adhesives. We have used Fourier transform infrared spectroscopy (FT-IR) and NMR to study the interaction of acetic acid with the surface of sodium aluminoborosilicate continuous glass fibers. Methods were developed that enable analyses to be carried out without damaging or altering the pristine as drawn fiber surface. While dosing the surface of fumed silica with acetic acid resulted in the formation of silyl ester groups, analogous dosing of sodium aluminoborosilicate glass fibers resulted in the formation of carboxylate species, principally coordinated to sodium, while silyl ester groups were not observed.

KEYWORDS: fiber • glass • FT-IR • CPMAS NMR • adhesive • carboxylic acid • surface chemistry • monolayer

1. INTRODUCTION

The creation of interfaces between oxide glass and polymers is pervasive in science, engineered coatings and composites, biotechnology, and even architecture (1−3). However, our understanding of the chemical bonding structure at those interfaces and the magnitude and stability of the adhesion it generates is limited. It is commonly assumed that silanol groups at the glass surface are responsible for the formation of chemical bonds with functional groups in the polymer (4, 5). In the case of silicon dioxide and silica glass, such a reaction can occur in some cases, but the stability of the bond is reduced in humid environments. For this reason, silane coupling agents are commonly added to enhance the interface reactivity, to tailor the interface structure for specific properties, and to maintain adhesion in humid environments (6, 7). There have been many studies reported about the nature of the silica/polymer or silica/silane interface based upon adsorption and reaction of small molecules with high-surface-area silica (primarily, CAB-O-SIL) but vanishingly few for silicate glasses.

Of particular interest in this study is the interface between multicomponent silicate glasses and adhesive polymers (8, 9). Here too, polymer adhesives are applied directly to the glass surface in the presence or absence of a silane coupling agent, but in the case of multicomponent glasses, much less is known about the molecular interactions and structure at the glass surface, glass/polymer, or glass/silane interface. One reason for this lack of knowledge is the absence of a high surface area analog to CAB-O-SIL for multicomponent glasses that would facilitate the type of surface adsorption studies performed with silica (10−15). Another reason is the complexity of multicomponent silicate glass surfaces. The presence of aluminum oxide and boron oxide in the silicate network will influence the activity of the silanol groups and, at the same time, introduce new surface sites. More so, the sodium and other modifier ions at the silicate surface are reactive and mobile; they can react with or diffuse into the polymer and/or shield the formation of chemical bonds to the silicate, borate, and aluminate units that compromise the glass network.

In this study, a sodium aluminoborosilicate glass was used in the form of continuous glass fibers. The fibers were made in our laboratory (using a commercial composition) to provide freshly drawn surfaces for surface adsorption studies by Fourier transform infrared spectroscopy (FT-IR) and NMR. Due to the prevalence of carboxylic acid groups in many commercial adhesives and their potential to form silyl ester linkages to the silicate network and carboxylates with sodium (and other alkali or alkaline earth species in glass), small molecules such as acetic acid and acetyl chloride served as the primary adsorbates studied. Surface functionalization with fluorosilane was used to independently determine the "reactive" hydroxyl concentration at the glass surface (16). These experiments with the sodium aluminoborosilicate fibers were performed in parallel with experiments on powdered fumed silica to provide reference data

* Corresponding author. E-mail: jjs366@psu.edu.
Received for review August 13, 2010 and accepted October 18, 2010
† Materials Research Institute.
‡ Department of Chemistry.
§ Department of Materials Science and Engineering.
DOI: 10.1021/am100730z

to aid in uncovering the unique effects of sodium. Likewise, sodium was leached from the multicomponent glass surface using a strong acid to provide a surface with reduced sodium concentration. It was found that the presence of sodium, even at very low concentration, leads to the formation of carboxylates at the surface, while the formation of silyl esters (found in the case of pure silica) was not detected. It is not yet known whether the sodium (and perhaps other) carboxylates form bridges across the interface that contribute to the adhesion or simply consume interface area and, thereby, limit the formation of silyl esters.

2. EXPERIMENTAL SECTION

2.1. Materials. Sodium aluminoborosilicate glass fibers were drawn using a custom built fiber draw system. Bulk glass (commercial glass wool composition) was melted at 1000 °C in a single tip platinum−rhodium crucible and allowed to equilibrate for 1 h. The melted glass then passed through a 2 mm i.d. tip and was drawn at 4.6 m/s onto a Teflon cylinder. Fiber was drawn for 15 min under standard laboratory conditions (<25% RH and 25 °C) and analyzed immediately or stored under vacuum for future analyses. Under these conditions, fibers had an average diameter of approximately 5 μm.

CAB-O-SIL fumed silica (M5, Cabot Corporation, Billerica, MA) was used as received. Acetic acid (>99%, Sigma-Aldrich), acetyl chloride (>99%, Sigma-Aldrich), and potassium bromide (International Crystal Laboratories, Garfield, NJ) were used as received for all infrared (IR) studies. Isotopically enriched acetic acid-1-^{13}C (99 atom %, Sigma-Aldrich), acetyl chloride-1-^{13}C (99 atom %, Isotec), toluene (Sigma-Aldrich, 99.8%), and (3,3,3-trifluoropropyl)dimethylchlorosilane (TFS; Gelest, Inc.) were used as received for NMR studies. Leaching solutions were prepared using deionized water (>18MΩ) and 12.1 M hydrochloric acid (ACS grade, EMD Chemicals).

2.2. Characterization Methods. Infrared spectra were acquired on an IFS 66/s spectrometer (Bruker Optics, Billerica, MA) using a Collector II diffuse reflection accessory equipped with a high temperature/vacuum (HTV) sample chamber (Thermo Spectra-Tech, Madison, WI). The HTV cell was outfitted with CaF_2 windows (New Era Enterprises, Vineland, NJ) and operated under vacuum or purged with UHP Argon (Grade 5.0, PraxAir) that was further purified using an oxygen/moisture/hydrocarbon filter (Restek, Bellefonte, PA). Spectral intensities are reported as $-\log(R/R_0)$, where R is the reflectivity of the sample and R_0 is the reflectivity of a reference sample. All spectra were acquired by averaging 1600 scans at 6 cm^{-1} resolution using an MCT detector.

For NMR experimentation, glass or silica samples were packed into 4 mm (outer diameter) zirconia magic-angle spinning (MAS) rotors. All samples were maintained under nitrogen prior to and during analysis. ^{1}H−^{13}C cross-polarization MAS (CPMAS) NMR experiments were performed with high-power proton decoupling on a Bruker 7.0 T NMR Spectrometer operating at a ^{13}C irradiation frequency of 75.551 MHz and a ^{1}H frequency of 300.431 MHz. Experimental setup was performed using Bruker Topspin version 1.3 interfaced to a Bruker 4 mm double-resonance (DR) widebore MAS probe. All experiments were acquired for 16 000 transients with a total of 4096 complex points and 40 kHz bandwidth. CPMAS was achieved utilizing a ^{1}H $\pi/2$ pulse width of 5.18 μs, a contact time of 5 ms, a recycle delay of 5 s, and a MAS spinning rate of 5000 Hz.

Samples silylated with (3,3,3-trifluoropropyl)dimethylchlorosilane (TFS) were probed using ^{19}F MAS NMR. ^{19}F experiments were performed on a Tecmag 9.4 T NMR spectrometer operating at a ^{19}F Larmor frequency of 376.346 MHz interfaced with a 4 mm DR Chemagnetics probe. Experimental data sets were acquired with either 5000 or 50 000 transients depending upon signal intensity. For each sample, a total of 2048 complex points were acquired with a 50 kHz sweep width. ^{19}F MAS NMR was achieved utilizing a $\pi/2$ pulse width of 6 μs, a recycle delay of 5 s, and a MAS spinning rate of 10 000 Hz. All NMR data processing was performed using NUTS software (Acorn NMR Inc., Livermore, CA), and ^{13}C resonances are referenced via a secondary standard (solid hexamethybenzene) to TMS, while ^{19}F data are referenced to neat $CFCl_3$ via a secondary standard of sodium trifluoroacetate.

X-ray photoelectron spectroscopy (XPS) analyses were performed on a monochromatic Al Kα source instrument (Kratos, Axis Ultra, England). Spectra were collected with a photoelectron take off angle of 90° and a 40 eV pass energy. All spectra were referenced to the C 1s binding energy at 285.0 eV.

BET surface area analyses were performed using a Micromeritics ASAP 2020 (Micromeritics, Norcross, GA). Prior to nitrogen adsorption, the samples were degassed at 30 °C for 4 h under a vacuum of $\sim 1 \times 10^{-2}$ Torr.

2.3. In Situ Infrared Analyses. A number of reports have utilized infrared spectroscopy to study glass fiber surfaces (e.g., see Chapter Four of Nardin (17)). However, to the best of our knowledge, this is the first report describing the in situ characterization of glass fiber surface chemistry using infrared spectroscopy. To better understand the fundamental surface adsorption phenomena on glass fibers, it was necessary to develop a novel method for mounting samples in the HTV diffuse reflection chamber. Fibers needed to be mounted in a manner amenable to in situ heating and vapor dosing. Additionally, it was critical to handle fibers in a way such that the integrity of the as drawn surface was not compromised by spurious contamination or physical damage. Previous methodologies involving dispersion of glass fibers in infrared diluent materials such as KBr are precluded here as they present a competing surface for probe molecule adsorption.

We have developed a technique that uses a 3/8 in. stainless steel spiral retaining ring (McMaster-Carr, Chicago, IL) to secure neat fibers for diffuse reflection analyses. Mounting samples into the ring was accomplished by suspending fibers between the jaws of a small vice and securing their ends with small clamps. Fibers were drawn taut by the reverse action of the vice and using fine point tweezers; the spiral retaining ring was opened, brought around the fibers, and released. Excess fiber was then trimmed from the edges of the retaining ring to leave a collection of mostly aligned fibers suspended in the center of the ring. A typical loading of fibers was approximately 20 mg. The sample was then placed on top of the alumina cup in the HTV chamber and positioned such that the fibers were centered at the focal plane of the accessory.

Prior to and during dosing, fiber samples were heated at ∼125 °C (sample surface temperature) in vacuo to remove water. The presence of physisorbed water was monitored via the O−H stretching region of the infrared spectrum. After approximately 30 min, the chamber was switched to an argon purge for an additional 30 min. The HTV cell was pumped with a turbo pump capable of attaining a base pressure of approximately 1×10^{-6} Torr at the pump inlet. However, due to conductance issues and the intrinsic leak rate of the cell, the pressure in the sample chamber is certainly higher. As such, it was possible to attain a lower partial pressure of water vapor in the sample chamber by purging with dry argon rather than with active pumping. Gas phase probe molecules were delivered into the HTV via Teflon and stainless steel tubing by purging argon gas over the surface of the liquid contained within a glass dosing apparatus. The vapor dosing apparatus for IR measurements consisted of a 50 mL 3-neck glass flask with Teflon stopcocks on two necks, inlet and outlet ports. The third neck was used for transfer of the probe liquids into the flask within a nitrogen purged glovebag. Vapor phase species were intro-

duced by diverting the argon purge such that it passed over the liquid in the flask prior to entering the HTV chamber. Argon flow rates of 30−80 mL/min were typical. Dosing was monitored in real time using the spectrometer, when possible; peak(s) indicative of surface coordination were monitored. After approximately 10 min, a quasi-steady-state surface concentration was typically observed and dosing was stopped. A dose of this duration does not imply maximum coverage but rather that large changes in the peak intensity of observable surface species were no longer apparent. After dosing, the HTV was purged with argon to remove residual vapor phase species.

2.4. Vapor Phase Dosing of NMR Samples. Vapor dosing of NMR samples was carried out ex situ using a custom built dosing apparatus. This apparatus consisted of a roughing pump connected to a glass manifold with two separate chambers. The sample chamber was heated using an external furnace, and the second chamber held either acetic acid or acetyl chloride. Dosing of the sample surface was carried out by loading approximately 0.5 g of sample into the sample chamber and heating to 125 °C for 30 min under vacuum (~1×10^{-3} Torr). The vacuum valve was closed, and the dosing chamber was opened to expose the sample to the vapor of the probe molecules for up to 16 h. A parallel experiment was performed where dosing was carried out for approximately 30 min. The reduced dosing time yielded peaks of decreased intensity with similar position and width as compared to the 16 h dose. After dosing, the sample chamber was disconnected from the apparatus and placed in a N_2 purged glovebag. Samples were either stored under an atmosphere of N_2 or immediately packed into NMR rotors. All sample preparation including the packing and unpacking of rotors was performed under an inert nitrogen atmosphere utilizing a glovebag.

2.5. TFS Functionalization. Reactive surface hydroxyl groups were quantified using ^{19}F MAS NMR by functionalizing the sample surface with (3,3,3-trifluoropropyl)dimethylchlorosilane (TFS; Gelest, Morrisville, PA) (16, 18). Approximately 0.5 g of sample was heated to 160 °C for 16 h under vacuum (~1×10^{-3} Torr). The sample was cooled to 100 °C and placed in a Schlenk flask with 25 mL of toluene and 1 mL of TFS. The flask was evacuated and then purged with argon. The silylation reaction proceeded for 3 days at room temperature with constant stirring. After 3 days, the sample was vacuum filtered using dry toluene as a rinse and heated at 120 °C for 1 h to drive off physisorbed TFS.

3. RESULTS AND DISCUSSION

3.1. Adsorption on Fumed Silica. The characterization and surface chemical modification of silica has been widely studied, and several books are devoted to the review of the subject (4, 19, 20). For this reason, CAB-O-SIL, a high surface area fumed silica, was chosen as the reference oxide for this study. The fumed silica surface is composed of mostly isolated silanols with some geminal and vicinal groups (4). This homogeneous surface is ideal for studying the interaction of silanol groups with acetic acid. Furthermore, it provides an appropriate segue to begin correlating data from solid-state NMR and infrared spectroscopy experiments prior to investigating the sodium aluminoborosilicate surface.

Several reports have utilized infrared spectroscopy to investigate the interaction of acetic acid with silica (21−24). These reports attributed the appearance of a band in the 1740−1760 cm^{-1} region with the C═O stretching mode of a silyl ester species formed by the condensation of acetic acid with silanols. In many cases, physisorbed acetic acid

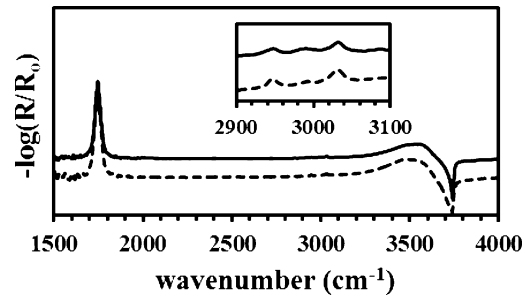

FIGURE 1. Infrared spectra of fumed silica dose with acetic acid (solid) and acetyl chloride (dashed). The spectra have been scaled to facilitate visualization.

was also present on the silica surface and a peak in the 1717−1724 cm^{-1} region was ascribed to the C═O stretching of molecular acetic acid hydrogen bound to a silanol (21−23). The systematic study by Young detailed the interaction of acetic acid, acetyl chloride, and acetic anhydride with fumed silica, and the presence of a carbonyl stretching mode in the 1740−1765 cm^{-1} range showed that in all cases a covalent silyl ester linkage formed (21).

Prior to dosing, the FT-IR fumed silica samples were heated to ~175 °C for 30 min to remove physisorbed water. Vapor dosing and spectral acquisitions were subsequently carried out at ~125 °C to minimize the presence of physisorbed acetic acid. Experiments carried out with the sample at room temperature have a peak at approximately 1720 cm^{-1} that can be assigned to physically adsorbed acetic acid. The diffuse reflection spectra of fumed silica after in situ exposure to acetic acid and acetyl chloride vapor are shown in Figure 1. These are plotted as differential absorbance spectra; i.e., a spectrum of the sample was acquired just prior to vapor dosing and used as the reference. Thus, the appearance of positive and negative peaks corresponds to the formation and loss of infrared active species relative to the predose state. Moreover, this presentation facilitates observation of small spectral changes related to surface adsorption phenomena which may otherwise go undetected in the presence of strong bulk vibrations. All spectra reported herein are presented in the differential absorbance format. Fumed silica is strongly absorbing below 1600 cm^{-1}, and as such, this region of the diffuse reflection spectrum was not useful. It is also possible to reference the predose and postdose spectra independently to a suitable reference such as KBr and then perform a spectral subtraction to acquire the difference spectrum. However, due to the duration of the measurements, it was difficult to perfectly correct for the influence of laboratory water vapor in the spectra. Qualitatively, the final spectra were the same using either method.

Inspection of Figure 1 reveals peaks at ~3500 cm^{-1}, 3032 cm^{-1} (C−H str.), 2988 cm^{-1} (C−H str.), 2947 cm^{-1}(C−H str.), and ~1745 cm^{-1} (C═O str.) with a corresponding negative peak centered at ~3738 cm^{-1} (loss of SiO−H str.) after dosing with acetic acid and acetyl chloride. These peak assignments are generally in agreement with the transmission FT-IR measurements reported for similarly functionalized discs of pressed fumed silica in which a silyl ester formed. However, the peak at 1745 cm^{-1}, as well as growth

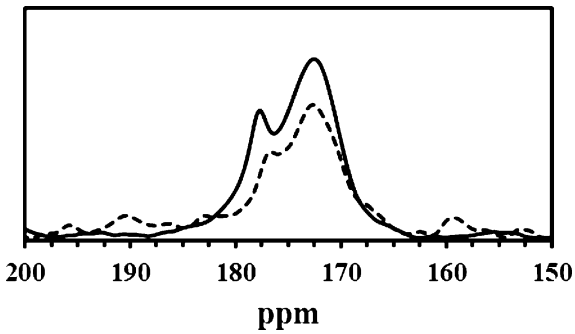

FIGURE 2. NMR of fumed silica dose with acetic acid (solid) and acetyl chloride (dashed).

of a band at ~3500 cm^{-1}, corresponds to a low coverage silyl ester monolayer where unreacted silanol groups hydrogen bond to the carbonyl group of the ester (21). The broad peak at ~3500 cm^{-1} is likely a combination of the Si(O−H) stretching of H-bonded silanols and/or (H−O)H stretching of molecular water.

The adsorption reactions of acetic acid and acetyl chloride on fumed silica were further investigated using CPMAS NMR. The $^{1}H-^{13}C$ CPMAS NMR spectra of fumed silica dosed with ^{13}C enriched acetic acid and ^{13}C enriched acetyl chloride at 125 °C are shown in Figure 2. In each case, the ex situ dosing of the silica surface resulted in the appearance of two peaks; both have a relatively broad peak centered at 172 ppm (8 ppm fwhm) and a narrower peak at 178 (4 ppm fwhm) and 176 ppm (3 ppm fwhm) for acetic acid and acetyl chloride, respectively. In general, the ^{13}C chemical shift for the carbonyl carbon in esters and carboxylic acids is typically between 160 and 185 ppm (25). More specifically, neat liquid samples of acetic acid and acetyl chloride display peaks at 178 and 170 ppm, respectively (26).

The 178 ppm peak on fumed silica after acetic acid dosing is equivalent in position to that of neat acetic acid. This suggests that in both cases acetic acid molecules possess sufficient mobility to maintain an isotropic orientation distribution. Additionally, dosing with acetic acid at approximately 200 °C resulted in a decrease in the intensity of the 178 peak relative to that at 172 ppm. In light of these observations, we attribute the peak at 178 ppm to acetic acid physisorbed on the silica surface. Correspondingly, the peak at 176 ppm in the acetyl chloride dosed sample is also assigned to physisorbed species likely consisting of both acetic acid and acetyl chloride. The hydrolytic sensitivity of the silyl ester bond has been reported in literature and observed in our FT-IR experiments (21). Furthermore, a companion FT-IR experiment confirmed this sensitivity. After in situ acetic acid dosing of fumed silica at 125 °C, a vacuum was pulled on the cell and the temperature dropped to 25 °C. The vacuum leak rate was sufficient to draw atmospheric moisture into the cell. Under these conditions, physisorbed acetic acid (new peak at 1715 cm^{-1}) formed at the expense of the silyl ester species (loss of peak at 1745 cm^{-1}). The observation of physisorbed species in all NMR experiments is partially related to trace amounts of water being present in the dosing system as either a byproduct of ester formation or a spurious contaminant. It should be noted that the sample pretreatment protocol was established to remove bulk water while trying to avoid modification of the native structure and chemistry of the as drawn fiber surface. Furthermore, the ex situ dosing and sample transfer protocol were meant to minimize exposure to water but rigorously anhydrous conditions are not guaranteed.

Table 1. Surface Composition by XPS of as Drawn and Leached Sodium Aluminoborosilicate Fibers after Acetic Acid Dosing

	Atomic Concentration (at %)								
	O	Na	Ca	Mg	K	C	B	Si	Al
as drawn	56	9	2	1	<1	12	2	15	2
leached	56	5	1	<1	<1	13	1	20	2

Liquid-state ^{13}C NMR experimentation on various poly(silyl ester)s report carbonyl frequencies at and around 172 ppm (27). In accordance with FT-IR observations, the 172 ppm peak observed on both the acetic acid and acetyl chloride dosed samples is ascribed to formation of a silyl ester. The assignment of this peak to a chemisorbed species is further supported by the relatively broad peak width that indicates the molecules have limited mobility and are less capable of rapid reorientations on the surface as a result of strong interactions with the oxide surface.

3.2. Adsorption on Sodium Aluminoborosilicate Fibers. The sodium aluminoborosilicate fiber possesses a more chemically heterogeneous surface as compared to fumed silica (see Table 1). Although the effects of sodium are the focus here and most evident in the data presented below, the other modifiers in the glass are expected to behave similarly. It can be seen in Figure 3 that acetic acid dosing of this surface resulted in a strong peak at 1573 cm^{-1} with no discernible peak appearing in the silyl ester region of the spectrum. It was not uncommon for the difference spectrum of the as drawn fiber to exhibit some sinusoidal features. We believe these features may be attributed to a slight perturbation in the physical position of the fiber after dosing relative to predosing. Given the small diameter of the fibers used here, it is possible that some infrared passes completely through the fiber before being reflected back out of the sample and setting up a condition which produces spectral artifacts similar to the interference fringes observed in some transmission measurements. A minor feature appears at 1695 cm^{-1} (intensity 0.05% that

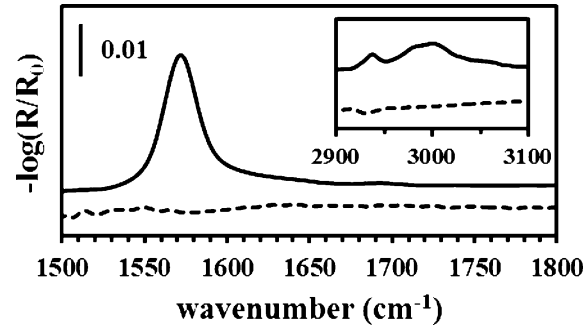

FIGURE 3. Infrared spectra of as drawn sodium aluminoborosilicate fiber dosed with acetic acid (solid) and acetyl chloride (dashed). Scale bar does not apply to inset.

of the 1573 cm^{-1} peak) that may be related to an additional surface species. However, given the aforementioned sinusoidal interference, we are not confident assigning this feature to any particular species. The inset in Figure 3 reveals the presence of C−H stretching modes (methyl group) at 3002, 2982, and 2937 cm^{-1} after dosing with acetic acid. Clearly, the surface chemistry has changed dramatically, compared to pure silica, even though this surface contains ~65 mol percent silica.

The 1573 cm^{-1} peak is assigned to the CO_2^- asymmetric stretching mode of an acetate species coordinated principally to sodium at the fiber surface. The CO_2^- asymmetric and symmetric stretching modes for anhydrous sodium acetate were first reported at 1578 and 1414 cm^{-1}, respectively (28). Since that report, there have been numerous experimental and computational studies investigating the vibrational spectrum of sodium acetate. A recent tabulation of experimental data for solid-state sodium acetate yields a range of 1580−1562 cm^{-1} for CO_2^- asymmetric stretching mode (29). Furthermore, computational studies have revealed that the CO_2^- symmetric and asymmetric stretching modes of sodium acetate are sensitive to the local environment. Optimized sodium acetate structures containing 1, 2, 3, or 4 water molecules reveals a shift in the CO_2^- stretching modes relative to the anhydrous structure. The calculated CO_2^- asymmetric stretching for a sodium acetate complex containing one water molecule is 1573 cm^{-1} (29). The intent of the predosing heat treatment was to remove physisorbed surface water without altering the intrinsic chemistry of the as drawn surface, but again, the complete elimination of water cannot be guaranteed. The absolute frequency of the CO_2^- asymmetric and symmetric stretching modes as well as the difference between them is often used to assign coordination type for carboxylate species (30). However, due to the strong reflectance of the fibers below 1500 cm^{-1}, the symmetric stretching mode corresponding to the 1573 cm^{-1} asymmetric stretch was indiscernible.

Both acetic acid and acetyl chloride possess the reactivity necessary to form ester linkages with silanol groups. The presence of chlorine on the carbonyl group makes acetyl chloride more reactive than acetic acid as an acylation reagent (31). However, acetyl chloride lacks the intrinsic structure necessary to form a carboxylate complex. Neither ester nor carboxylate species were observed in the spectrum after the fiber was dosed with acetyl chloride; see Figure 3. This observation further supports assignment of the 1573 cm^{-1} peak to the presence of a carboxylate species. Furthermore, sodium is approximately 4 times more abundant in the near surface region of the fiber than other elements capable of participating in carboxylate complex formation (Table 1).

While coordination with sodium is the principal interaction, some interaction with calcium and/or aluminum cannot be entirely ruled out given their concentration in the near surface region. Lee et al. studied the interaction of oleic acid with a soda lime silicate glass powder and assigned the CO_2^- asymmetric stretching of a carboxylate group coordinated

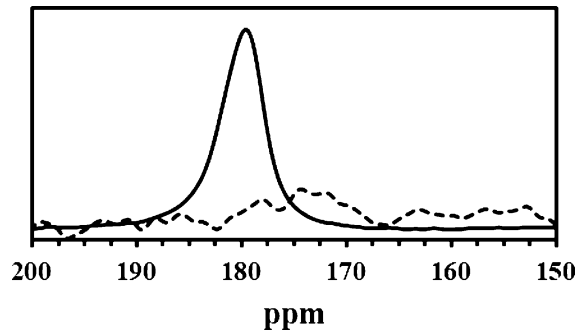

FIGURE 4. NMR spectra of as drawn sodium aluminoborosilicate fiber dosed with acetic acid (solid) and acetyl chloride (dashed).

to sodium, calcium, and aluminum to peaks appearing at 1558, 1581, and 1600 cm^{-1}, respectively (32). However, differences in our glass composition, sample preparation, and the sensitivity of the CO_2^- asymmetric stretching mode to its local environment make a direct correlation with these peak positions tenuous. The asymmetry of the peak centered at 1573 cm^{-1} may permit deconvolution; however, this was not pursued given the lack of suitable reference data from which accurate fitting parameters could be developed.

The $^1H-^{13}C$ CPMAS NMR spectra of as drawn sodium aluminoborosilicate fiber dosed with ^{13}C enriched acetic acid and ^{13}C enriched acetyl chloride at 125 °C are shown in Figure 4. In agreement with the FT-IR, there is little evidence for the formation of silyl esters (only a minuscule bump appears at 172 ppm in the spectrum) or any other surface reaction product when the sample is dosed with acetyl chloride. However, when the fiber surface is dosed with acetic acid, a large peak appears at 180 ppm (fwhm 5 ppm), and this peak is shifted from where resonances appeared for both the silyl ester and physisorbed acetic acid species. On the basis of the FT-IR and XPS results, this peak is ascribed to formation of a sodium acetate complex.

3.3. Adsorption on Acid Leached Sodium Aluminoborosilicate Fibers. Sodium has been shown to play a central role in the adsorption of acetic acid on the surface of the sodium aluminoborosilicate fibers. To further evaluate the effects of sodium on acetic acid adsorption, the near surface sodium concentration was reduced via acid leaching. The fibers were leached in a 50 °C, pH 3 (HCl acidified) aqueous solution for approximately 60 s and then rinsed with several aliquots of 50 °C deionized water. Excess water was removed by blotting the fibers with lint free tissue prior to analysis. Analogous to the FT-IR experiments with as drawn fiber, the leached fibers were heated at 125 °C under vacuum and argon to remove water prior to acetic acid dosing.

The XPS compositional analyses of acid leached sodium aluminoborosilicate fibers after acetic acid dosing are shown in Table 1. These analyses were performed after acetic acid dosing because ancillary experiments revealed that the heating intrinsic to our dosing experiments was sufficient to replenish some sodium in the near surface region. Even with thermally induced redistribution, the sodium and calcium concentrations were typically half that of the as drawn fiber while aluminum was largely unaffected. The higher Si

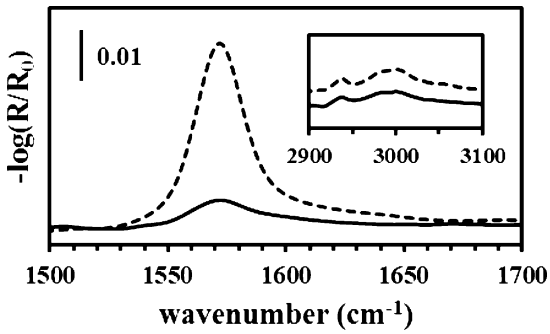

FIGURE 5. Infrared spectra of as drawn (dashed) and leached (solid) sodium aluminoborosilicate fiber dosed with acetic acid. Scale bar does not apply to inset.

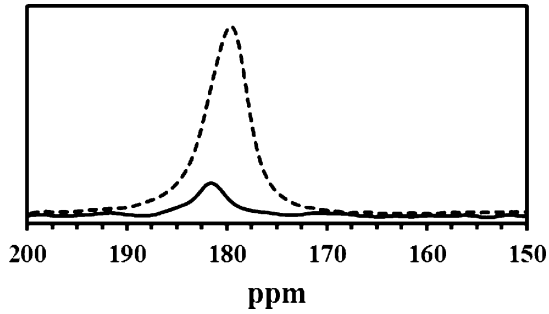

FIGURE 6. NMR of as drawn (dashed) and leached (solid) sodium aluminoborosilicate fiber dosed with acetic acid.

concentration on the leached surface is further evidence that the leached surface is unique relative to the as drawn surface.

FT-IR spectra of leached and as drawn fibers, after dosing with acetic acid, are compared in Figure 5. Commensurate with the reduction of sodium, there was a marked decrease in the intensity of the 1573 cm^{-1} sodium carboxylate peak after leaching. The C−H stretching regions of the as drawn and leached fibers are qualitatively similar (see inset Figure 5). Similarly, the $^{1}H-^{13}C$ CPMAS NMR spectrum of leached fiber, shown in Figure 6, displays a dramatic decrease in the intensity of the sodium carboxylate peak at 180 ppm. Altogether, these observations confirm a correlation between the surface sodium concentration and the extent of carboxylate formation.

It can also be expected that a reduction in surface sodium concentration might enhance coordination with other metal constituents in glass. Lee and Condrate found that more stable carboxylate species can form when Al, Ca, and Mg are present (32−35). The asymmetric CO_2^- stretching mode for carboxylic acids adsorbed on alumina and oxidized aluminum surfaces has been reported in the 1583−1608 cm^{-1} region (32, 36−38). Furthermore, the intensity ratio of the shoulder centered at ∼1595 cm^{-1} to the peak at 1573 cm^{-1} increased by a factor of approximately two after leaching. As such, the broad shoulder centered at ∼1595 cm^{-1} is largely ascribed to the formation of aluminum carboxylate species. Given the breadth of the shoulder at ∼1595 cm^{-1}, calcium carboxylate species are possible (although the formation of calcium carboxylate species should result in multiple peaks in both the FT-IR and NMR spectra 35, 39−41), but clearly, the most important outcome of these experiments on the leached fiber was the absence of silyl ester formation in either the FT-IR or NMR spectra, even though the relative silica concentration on the leached surface increased (and thereby shielding of silanols by sodium is decreased). This indicates that the reduced reactivity toward ester formation on both the as drawn and leached surfaces is due to some factor other than physical shielding of surface silanols by sodium.

3.4. Quantification of Reactive Silanol Groups. Infrared spectroscopy and NMR have shown that silanol groups are the surface species reacting with acetic acid and acetyl chloride to form a silyl ester. Using a ^{19}F probe molecule to which NMR is highly sensitive, the number of reactive hydroxyl sites on silica or glass has been quantified by first reacting the surface with (3,3,3-trifluoropropyl)dimethylchlorosilane (TFS). The number of detected reactive silanol groups was normalized to the measured BET surface area of each sample to yield the number of reactive surface silanols per nm^2. The reactive hydroxyl number measured for fumed silica was found to be detectable at a concentration less than 1 OH/nm^2. Conversely, the amount of ^{19}F signal observed for the sodium aluminoborosilicate glass sample, even after 50 000 transients, remained only slightly above the level of noise for the as drawn fiber sample. A qualitative peak fit of the as drawn fiber ^{19}F spectrum reveals an approximate 500-fold reduction in the number of reactive silanol groups as compared to fumed silica. Clearly, the difference in reactivity of the TFS with these surfaces mirrors the behavior of the acetic acid.

For interpretation of these results, it should be noted that the TFS probe molecule is assumed to react selectively with nonhydrogen-bonded silanol groups on the surfaces of oxides. Using the usual Q^n notation, where *n* denotes the number of bridging oxygen's from a central four-coordinated atom to other network-forming species, it has been determined that TFS chemisorbs to isolated Q^3 groups. This conclusion based on previous investigations demonstrating that bonding between chlorosilanes and silanols and/or aluminols on mesoporous silica (42−44), amorphous silica (45, 46), and amorphous alumina (47, 48) occurs preferentially at nonhydrogen bonded lone hydroxyls. Zhao et al. (44) further hypothesized that intrasurface hydrogen bonding between silanol groups functions as a hydrophilic barrier. Supporting this hypothesis is the work of Kawai et al., which showed that areas of extensive H-bonding on aluminum-containing zeolites created "hydroxy nests" that were unreactive to condensation with chlorosilanes (42, 43). On the basis of these observations, we conclude that TFS attaches specifically to accessible nonhydrogen bonded species on the surfaces of fumed silica and the sodium aluminoborosilicate fibers, and for these species to be reactive, they must lie outside of any hydrogen-bonding network formed at the interface by the interaction of neighboring hydroxyl groups and any remaining proximal water (49−52). We, therefore, interpret the lower reactive hydroxyl numbers measured here (when compared to other estimates of hydroxyl density on silicate surfaces) to be the result of selective binding to

lone (isolated, freely vibrating) hydroxyl species. We hypothesize further that these lone hydroxyl species are then also the dominant formation sites for silyl ester reaction products. The lack of reactive species for silyl ester formation on the aluminoborosilicate fibers then does not mean that there are no hydroxyl species on the surfaces but that the number of reactive (i.e., lone) hydroxyl species is many orders of magnitude lower than those found on the fumed silica surface. To be sure, the leached surface has many more hydroxyls than the as drawn surface, but the majority are hydrogen bonded to one another at the surface where ester formation could otherwise occur.

4. CONCLUSIONS

We have used FT-IR and NMR to study the interaction of acetic acid with the surface of sodium aluminoborosilicate continuous glass fibers. Acetic acid was selected as a probe molecule representative of the carboxylic acid functional groups found in many adhesives. It is certain that the reaction products from acetic acid adsorption are different on sodium aluminoborosilicate glass surfaces compared to pure silica. On silica, silyl ester linkages can be detected, whereas on the multicomponent silicate, sodium (and perhaps other) carboxylates form in preference to ester linkages. We attribute this difference to the absence of isolated silanols, free of hydrogen bonding to other hydroxyls or water, on the multicomponent surface. The consequences of this reaction, at the interface of sodium aluminoborosilicate glass and an adhesive polymer containing carboxylic acid groups, are currently under investigation.

Acknowledgment. This material is based upon work supported by the National Science Foundation under Grant No. CHE-0809657. This work was also supported by the Pennsylvania State University Materials Research Institute Nanofabrication Lab and the National Science Foundation Cooperative Agreement No. 0335765, National Nanotechnology Infrastructure Network, with Cornell University.

REFERENCES AND NOTES

(1) Kwei, T. K. *Interfaces in Polymer, Ceramic, and Metal Matrix Composites*; Elsevier: New York, 1988; p 780.
(2) Mittal, K. L., Ed. *Silanes and Other Coupling Agents*; VSP: Utrecht, 2000; Vol. 2, pp 292.
(3) Wang, Y. Q.; Chen, J.; Gao, F.; Sherwood, P. M. A. *Surf. Interface Anal.* **2009**, *41*, 463–470.
(4) Iler, R. K. *The Chemistry of Silica: Solubility, Polymerization, Colloid and Surface Properties, and Biochemistry*. Wiley: New York, 1979.
(5) Berquier, J. M.; Arribart, H. *Langmuir* **1998**, *14*, 3716–3719.
(6) Plueddemann, E. P. *Silane Coupling Agents*, 2nd ed.; Plenum Press: New York, 1991.
(7) Pern, F. J.; Jorgensen, G. J. Enhanced Adhesion of EVA Laminates to Primed Glass Substrates Subjected to Damp Heat Exposure. In *31st IEEE Photovoltaics Specialists, NREL/CP-520−37391*, Lake Buena Vista, FL, 2005.
(8) Gappert, G.; Nakatani, A.; Weinstein, B. *Int. Nonwovens J.* **2005**, *14*, 2–10.
(9) Banerjee, J.; Hamilton, J. P.; Mueller, K. T.; Pantano, C. G., to be submitted for publication.
(10) Morrow, B. A.; Cody, I. A. *J. Phys. Chem.* **1975**, *79*, 761–762.
(11) Hair, M. L. *Infrared Spectroscopy in Surface Chemistry*; M. Dekker: New York, 1967.
(12) Morrow, B. A.; Cody, I. A. *J. Phys. Chem.* **1976**, *80*, 1995–1998.
(13) Morrow, B. A.; Cody, I. A. *J. Phys. Chem.* **1976**, *80*, 1998–2004.
(14) Morrow, B. A.; Cody, I. A.; Lee, L. S. M. *J. Phys. Chem.* **1976**, *80*, 2761–2767.
(15) Morrow, B. A.; McFarlan, A. J. *J. Non-Cryst. Solids* **1990**, *120*, 61–71.
(16) Fry, R. A.; Tsomaia, N.; Pantano, C. G.; Mueller, K. T. *J. Am. Chem. Soc.* **2003**, *125*, 2378–2379.
(17) Nardin, M., Papirer, E., Eds. *Powders and Fibers: Interfacial Science and Applications*; CRC Press/Taylor & Francis: Boca Raton, FL, 2007; p 660.
(18) Fry, R. A.; Mueller, K. T.; Pantano, C. G. *Phys. Chem. Glasses* **2004**, *45*, 222–222.
(19) Vansant, E. F.; Van der Voort, P.; Vrancken, K. C. *Characterization and Chemical Modification of the Silica Surface*; Elsevier: Amsterdam; New York, 1995.
(20) Papirer, E., Ed. *Adsorption on Silica Surfaces*; Marcel Dekker: New York, 2000; p 753.
(21) Young, R. P. *Can. J. Chem.* **1969**, *47*, 2237–2247.
(22) Hill, W.; Miessner, H.; Ohlmann, G. *J. Chem. Soc., Farady Trans. I* **1989**, *85*, 691–697.
(23) Horr, T. J.; Ralston, J.; Smart, R. S. *Colloids Surf.* **1992**, *63*, 21–28.
(24) Jackson, S. D.; Kelly, G. J.; Lennon, D. *React. Kinet. Catal. Lett.* **2000**, *70*, 207–212.
(25) Silverstein, R. M.; Bassler, G. C.; Morrill, T. C. *Spectrometric Identification of Organic Compounds*. 5th ed.; Wiley: New York, 1991.
(26) Spectral Database for Organic Compounds. http://riodb01.ibase.aist.go.jp/sdbs/cgi-bin/cre_index.cgi?lang=eng (accessed 07/15).
(27) Wang, M.; Weinberg, J. M.; Wooley, K. L. *Macromolecules* **1998**, *31*, 7606–7612.
(28) Jones, L. H.; McLaren, E. *J. Chem. Phys.* **1954**, *22*, 1796–1800.
(29) Tafipolsky, M.; Schmid, R. *J. Chem. Theory Comput.* **2009**, *5*, 2822–2834.
(30) Deacon, G. B.; Phillips, R. J. *Coord. Chem. Rev.* **1980**, *33*, 227–250.
(31) Smith, M.; March, J. *March's Advanced Organic Chemistry: Reactions, Mechanisms, and Structure*. 5th ed.; John Wiley: New York, 2001.
(32) Lee, D. H.; Condrate, R. A.; Lacourse, W. C. *J. Mater. Sci.* **2000**, *35*, 4961–4970.
(33) Lee, D. H.; Condrate, R. A. *J. Non-Cryst. Solids* **1997**, *222*, 435–441.
(34) Jang, H. K.; Whangbo, S. W.; Chung, Y. D.; Kim, T. G.; Kim, H. B.; Lyo, I. W.; Whang, C. N.; Wang, C. H.; Choi, D. J.; Kim, T. K.; Lee, H. S. *J. Vac. Sci. Technol., A: Vac. Surf. Films* **2000**, *18*, 2394–2399.
(35) Lee, D. H.; Condrate, R. A. *J. Mater. Sci.* **1999**, *34*, 139–146.
(36) Allara, D. L.; Nuzzo, R. G. *Langmuir* **1985**, *1*, 52–66.
(37) Kiselev, A. V.; Lygin, V. I. *Infrared Spectra of Surface Compounds*. Wiley; distributed by Halsted Press: New York, 1975.
(38) Evans, H. E.; Weinberg, W. H. *J. Chem. Phys.* **1979**, *71*, 4789–4798.
(39) Mielczarski, J. A.; Cases, J. M.; Tekely, P.; Canet, D. *Langmuir* **1993**, *9*, 3357–3370.
(40) Balimann, G. E.; Groombridge, C. J.; Harris, R. K.; Packer, K. J.; Say, B. J.; Tanner, S. F. *Philos. Trans. R. Soc. London Ser. A: Math. Phys. Eng. Sci.* **1981**, *299*, 643–663.
(41) Bryant, R. G.; Chacko, V. P.; Etter, M. C. *Inorg. Chem.* **1984**, *23*, 3580–3584.
(42) Kawai, T.; Tsutsumi, K. *Colloid Polym. Sci.* **1998**, *276*, 992–998.
(43) Kawai, T.; Tsutsumi, K. *J. Colloid Interface Sci.* **1999**, *212*, 310–316.
(44) Zhao, X. S.; Lu, G. Q. *J. Phys. Chem. B* **1998**, *102*, 1556–1561.
(45) Van-Der-Voort, P.; Gillis-D'Hamers, I.; Vansant, E. F. *J. Chem. Soc., Faraday Trans.* **1990**, *86*, 3751–3755.
(46) Lochmuller, C. H.; Kersey, M. T. *Langmuir* **1988**, *4*, 572–578.
(47) Paul, K.; Kubicki, J. D.; Sparks, D. L. *Environ. Sci. Technol.* **2006**, *40*, 7717–7724.
(48) Paul, K.; Kubicki, J. D.; Sparks, D. L. *Eur. J. Soil Sci.* **2007**, *58*, 978–988.
(49) Schlegel, M. L.; Nagy, K. L.; Fenter, P.; Sturchio, N. C. *Geochim. Cosmochim. Acta* **2002**, *66*, 3037–3054.
(50) Yang, J.; Meng, S.; Xu, L.; Wang, E. G. *Phys. Rev. B* **2005**, *71*, 035413-1–035413-12.
(51) Yang, J.; Meng, S.; Xu, L. F.; Wang, E. G. *Phys. Rev. Lett.* **2004**, *92*, 146102−1146102−4.
(52) Du, Q.; Freysz, E.; Shen, Y. R. *Phys. Rev. Lett.* **1994**, *72*, 238–241.

AM100730Z